AGU PUBLICATIONS

Geophysical Research Letters

RESEARCH LETTER
10.1002/2016GL071652

Key Points:
- Ceres shows extended spectrally blue-sloped regions similar to B-type asteroids
- Ceres's blue-sloped material is closely related to morphologically fresh impact craters
- Blue slope may be caused by changing physical properties (grain size/crystallinity) due to brecciation, grinding, and amorphization/melting

Correspondence to:
K. Stephan,
Katrin.Stephan@dlr.de

Citation:
Stephan, K., et al. (2017), An investigation of the bluish material on Ceres, *Geophys. Res. Lett.*, *44*, 1660–1668, doi:10.1002/2016GL071652.

Received 22 OCT 2016
Accepted 3 FEB 2017
Accepted article online 7 FEB 2017
Published online 18 FEB 2017

An investigation of the bluish material on Ceres

K. Stephan[1], R. Jaumann[1,2], K. Krohn[1], N. Schmedemann[2], F. Zambon[3], F. Tosi[3], F. G. Carrozzo[3], L. A. McFadden[4], K. Otto[1], M. C. De Sanctis[3], E. Ammannito[5], K.-D. Matz[1], T. Roatsch[1], F. Preusker[1], C. A. Raymond[6], and C. T. Russell[5]

[1]DLR, Institute of Planetary Research, Berlin, Germany, [2]Department of Earth Sciences, Institution of Geosciences, Free University of Berlin, Berlin, Germany, [3]INAF-IAPS, National Institute for Astrophysics, Rome, Italy, [4]NASA Goddard Space Flight Center, Greenbelt, Maryland, USA, [5]Institute of Geophysics and Planetary Physics, UCLA, Los Angeles, California, USA, [6]Jet Propulsion Laboratory, California Institute of Technology, Pasadena, California, USA

Abstract The dwarf planet Ceres shows spatially well-defined regions, which exhibit a negative (blue) spectral slope between 0.5 and 2.5 μm. Comparisons with planetary bodies known to exhibit a blue slope and spectral properties of materials identified on Ceres's surface based on infrared wavelength signatures indicate that the spectral changes could be related to physical properties of the surface material rather than variations in its composition. The close association of bluish surface regions to fresh impact craters implies a possible relationship to an impact-triggered alteration and/or space weathering processes. The bluish regions could be linked with blankets of ultrafine grains and partly amorphous phyllosilicates, which form larger agglomerates due to the sticky behavior of impact-induced phyllosilicate dust and/or the amorphization of the ejecta material during the impact process. Space weathering processes (micrometeoritic impacts, temperature changes) cause a reversal of the agglutination process and a recrystallization of the surface material with time resulting in a reddening of the spectral slope.

1. Introduction

Since NASA's *Dawn* spacecraft arrived at Ceres in March 2015, its Visible and Infrared Spectrometer (VIR) experiment [*De Sanctis et al*., 2011] has shown that the surface composition of Ceres, with a diameter of 945 km, the largest object in the asteroid belt, is dominated by a mixture of ammoniated phyllosilicates, Mg-phyllosilicates, and carbonates [*De Sanctis et al*., 2015]. A dark spectrally neutral material causes the overall low albedo of Ceres surface material [*De Sanctis et al*., 2015]. The composition has been found to be rather homogeneous on a global scale implying a globally widespread endogenous formation of the surface material, i.e., an aqueous alteration of silicates [*Ammannito et al*., 2016]. In contrast, the abundance of the individual surface compounds appears to be variable, which has been interpreted as evidence for a vertically stratified upper crust [*Ammannito et al*., 2016].

The VIR-derived composition, however, does not explain color variations observed in the visible spectral range. Color images returned by *Dawn*'s Framing Camera (FC) [*Sierks et al*., 2011] show extended regions of spectrally blue-sloped material (hereafter referred as bluish color) especially in the vicinity of morphologically fresh impact craters and their ejecta, while geologically old regions are characterized by spectrally red-sloped color (hereafter reddish/brownish color) [*Jaumann et al*., 2016]. Although rare, spectrally negative (blue) slopes have been measured on several planetary bodies such as B-type asteroids [*Clark et al*., 2010] as well as some icy satellites of Jupiter and Saturn [*Clark et al*., 2012; *Jaumann et al*., 2008; *Schenk and McKinnon*, 1991; *Stephan*, 2006] in addition to some carbon-rich meteorites [*Cloutis et al*., 2013], possibly caused by compositional and/or physical properties of the surface material. *Dawn* data from dwarf planet Ceres provide the unique opportunity to investigate the spectral nature of the bluish material in combination with their geologic and topographic context, which could be essential to solve its origin, further our understanding of Ceres's formation and geological evolution, and finally may offer implications for the existence of blue-sloped material on other planetary bodies.

2. Data and Processing

The bluish regions on Ceres's surface are best visible in the ratio of images acquired by *Dawn*'s Framing Camera (FC) [*Sierks et al*., 2011] using the filters F8 and F3 centered at the wavelengths 438 nm and 749 nm, respectively. The ratio of two channels represents the relation between two similar magnitudes, i.e., the

reflectance of each channel. Changes in the ratios are caused by changes in the spectral slope without a significant effect of the viewing geometry. A ratio <1 indicates a red (positive) slope because the reflectance increases toward longer wavelengths, and a ratio >1 implies a bluish (negative) slope with the reflectance decreasing toward longer wavelengths. The processing of FC data including radiometric calibration, photometric, and geometric correction is described in *Roatsch et al*. [2016] and *Schröder et al*. [2017]. Further, the high spatial ground resolution of the FC images of 35 m per pixel enables the detailed investigation of the geological context of the regions of interest and corresponding Digital Terrain Models (DTMs) derived from FC images by *Preusker et al*. [2016] are available to investigate the relationship to Ceres's surface topography.

In order to investigate the nature of the bluish material in detail, we included corresponding high spectral resolution data cubes acquired by the VIR spectrometer [*De Sanctis et al*., 2011] in our analysis, which detects Ceres's surface between 0.25 and 1.05 μm (VIR-VIS) as well as between 1.0 and 5.1 μm (VIR-IR), respectively. However, because of open calibration issues, we excluded the spectral information shortward of 0.4 μm. VIR observations offer a nominal ground resolution up to 90 m per pixel enabling the detailed correlation of spectral signatures to geological and/or morphological surface features. VIR observations have been radiometrically calibrated by the VIR team, and the IR signal has been thermally corrected following the procedure of *Tosi et al*. [2014]. Spectral parameters like the band depths (BDs) of individual absorptions [*Ammannito et al*., 2016] such as the absorptions at ~2.73 μm and ~3.1 μm attributed to ammoniated phyllosilicates, which dominate Ceres's overall spectral properties [*Ammannito et al*., 2016] have been derived. Carbonates appear to be common on Ceres as well causing absorptions centered near 2.2, 3.3–3.5, and 3.95 μm [*De Sanctis et al*., 2016]. Locally, Ceres spectra may show distinct absorptions at 1.5 and 2 μm, indicative of H_2O ice [*Combe et al*., 2016]. In addition, the ratio of the VIR channels at 1.1 and 2.5 μm has been used to check if the changes in the spectral slope implied by the FC data continue into the infrared wavelength region.

3. Spectral and Geological Characterization of the Blue Material

The global classification map of the spectral slope between the FC filters F8 (438 nm) and F3 (749 nm) (Figure 1) shows distinct patches of bluish material distributed across Ceres's surface. The ratio values vary between <1 (red slope) and >1 (blue slope). The corresponding VIR average spectra, which have been measured for each major slope class (Figure 1), show a reflectance maximum around 0.5 μm with the spectral continuum decreasing toward the UV as well as into the NIR up to 2.6 μm in the bluish areas. In contrast, the VIR spectra of the red regions exhibit a less marked reflectance maximum at longer wavelengths (~0.64 μm).

The bluish patches gradually change into the nonblue regions. The bluish color is closely related to morphologically fresh impact craters. The steepest blue slope has been measured for *Oxo* (diameter: 10 km; 42.2°N/359.6°E), *Haulani* (diameter: 34 km; 5.8°N/10.8°E) and the small impact crater *Tawals* (diameter: 8.8 km; 39.1°S/238°E). Prominent surface features, like *Occator* (diameter: 92 km; 19.8°N/239.3°E) and *Ahuna Mons* (diameter: 20 km; 10.5°S/316.2°E) as well as *Juling* (diameter: 20 km; 35.9°S/168.5°E) and *Kupalo* (diameter: 26 km; 6.7°S/218.4°E) still show a blue, but distinctly less steep, slope.

Geologically older surface features such as *Ikapati* (diameter: 50 km; 33.8°N/45.6°E), *Gaue* (diameter: 80 km; 30.8°N/86.2°E), *Azacca* (diameter: 77 km; 18.3°N/193.8°E), and *Dantu* (diameter: 126 km; 24.3°N/138.2°E) [*Hiesinger et al*., 2016; *Schmedemann et al*., 2016] are indicated by a more neutral spectral slope. The oldest heavily cratered regions on Ceres, such as in the vicinity of the impact crater *Sintana* (diameter: 58 km; 48.1°S/46.2°E), show a distinct reddish spectral signature. Linear features that cross Ceres's surface for hundreds of kilometers also show a bluish signature (because of the spatial resolution they only appear green in the classification map of Figure 1), which sometimes appear to be radial to large craters and thus were interpreted to be ejecta material [*Buczkowski et al*., 2016].

Figures 2 and 3 show type localities of bluish material. In the case of *Oxo*, the blue material is clearly associated with the crater itself and its ejecta deposits (Figures 2a–2f). The steepest blue slopes are confined to the crater wall. The relatively sharp border between ejecta and surroundings is defined by the local morphology, i.e., due to the topographic heights surrounding the crater. Oxo is located within an older and larger impact basin. In comparison with the geologically older surroundings, the blue-sloped ejecta of Oxo look morphologically very smooth. Close to the crater rim relatively large blocks are apparent (Figure 2f). The blue material exposed at the crater wall implies its excavation from the subsurface. The visual albedo of Oxo (= 0.084) [*Schmedemann et al*., 2016] is relatively high [*Combe et al*., 2016]. VIR data show weak

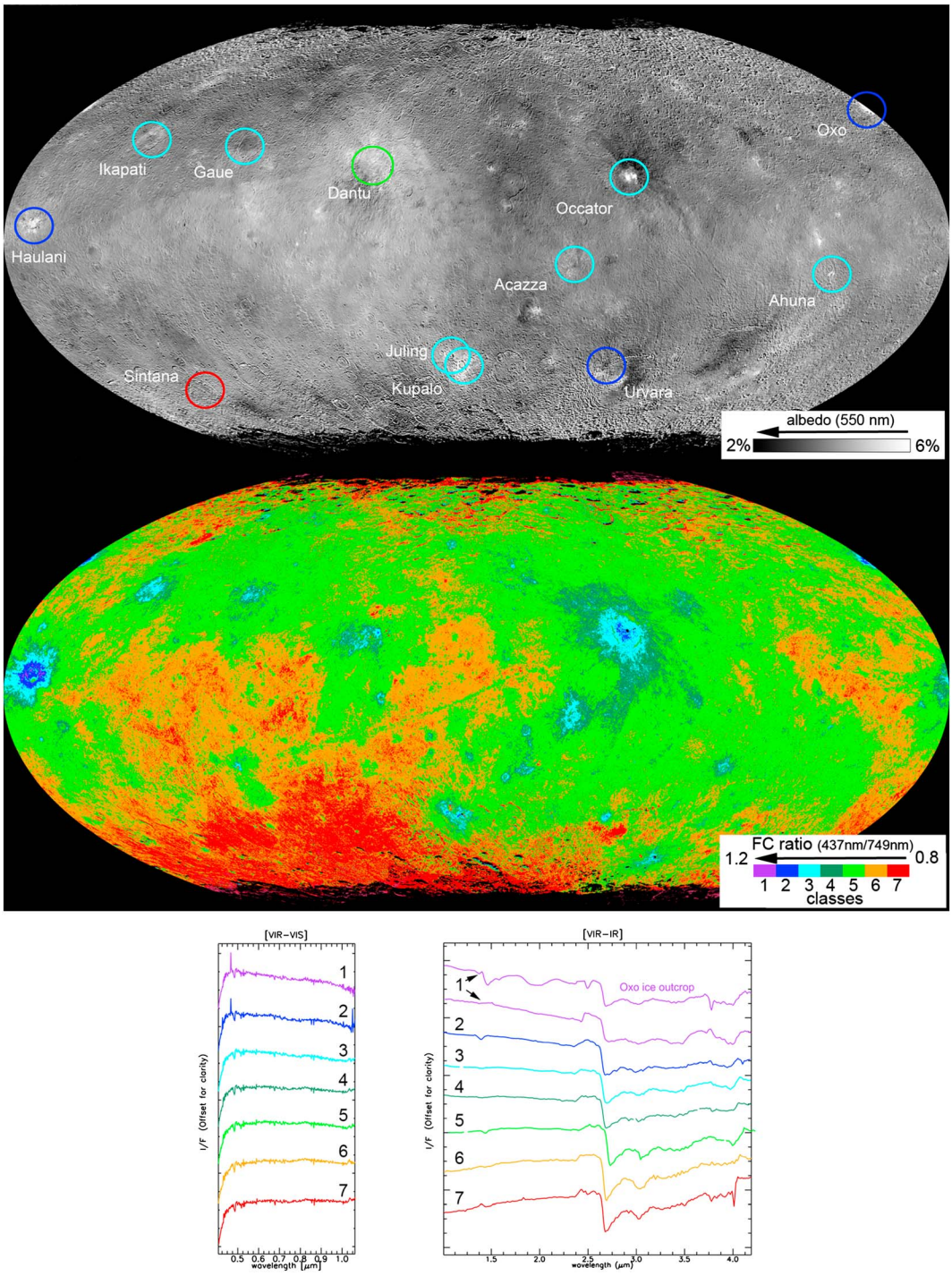

Figure 1. (top) Global geometric albedo at 550 nm, (middle) classification map of Ceres's F8/F3 ratio values, and corresponding (bottom left) VIR VIS and (bottom right) IR spectra. The positions of type localities are indicated by circles and colored as the corresponding slope class. Note that class 1 is represented by two spectra showing the same blue slope with one representing the outcrop of H_2O ice in impact crater Oxo.

absorptions at 2.7 and 3.1 μm in the area of crater Oxo and its ejecta, which correspond to those areas exhibiting the bluest slope. The exposure of H_2O ice as detected by *Combe et al.* [2016] due to the distinct H_2O-ice absorptions at 1.5 and 2 μm is only limited to a very local spot in the southern crater wall of Oxo, which is included in the blue-sloped area (Figure 2e).

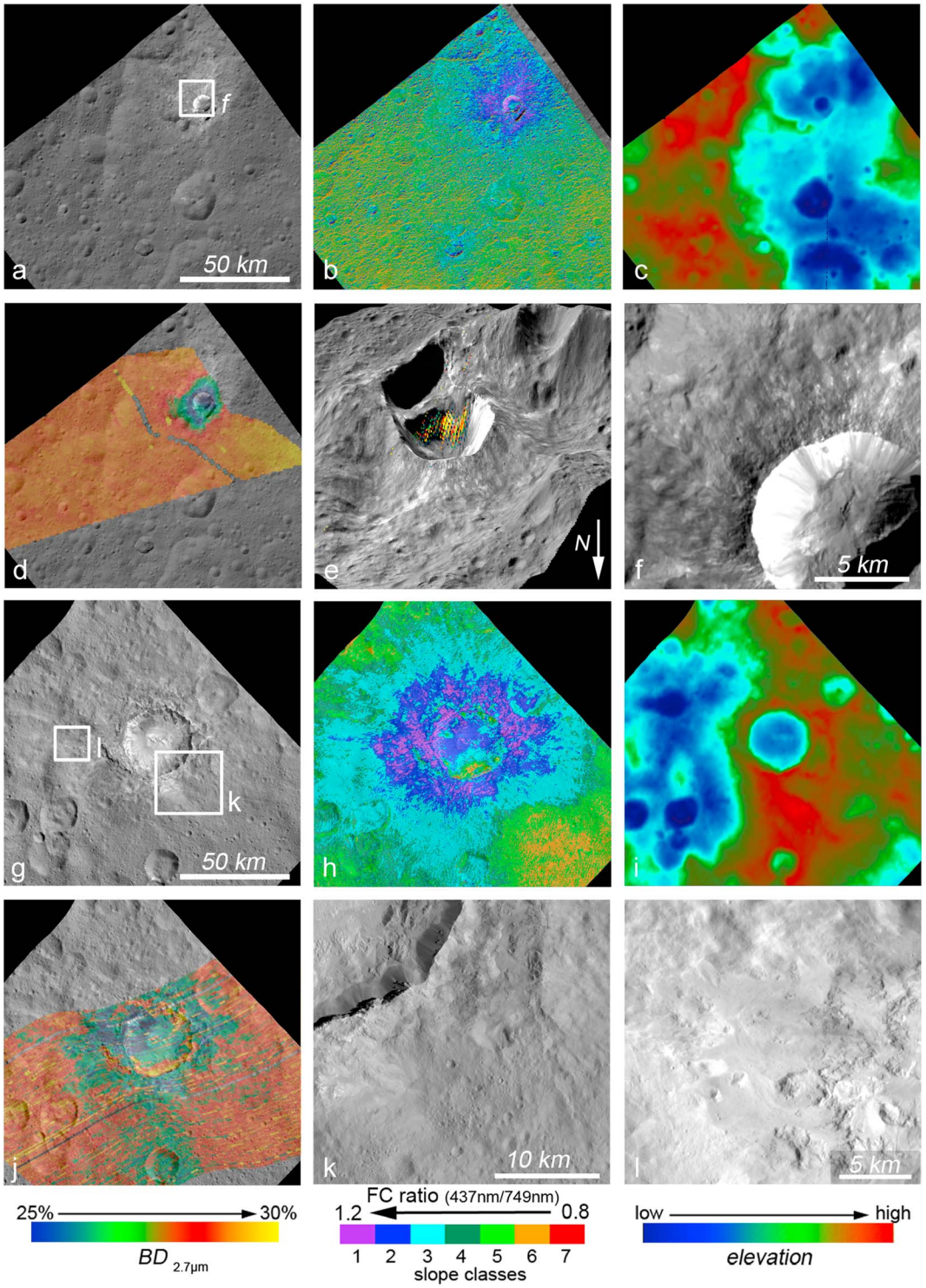

Figure 2. Type localities of blue material: (a) FC image of Oxo, and the corresponding (b) slope classification map (like in Figure 1), (c) DTM, (d) VIR derived *BD* 2.7 μm map, (e) 3-D view illustrating where H_2O ice has been detected, (f) close up FC image of blue ejecta material, (g) FC image of impact crater Haulani, and the corresponding (h) slope classification map, (i) DTM, (j) VIR-derived BD 2.7 map, and (k and l) close up FC images of blue-sloped ejecta material.

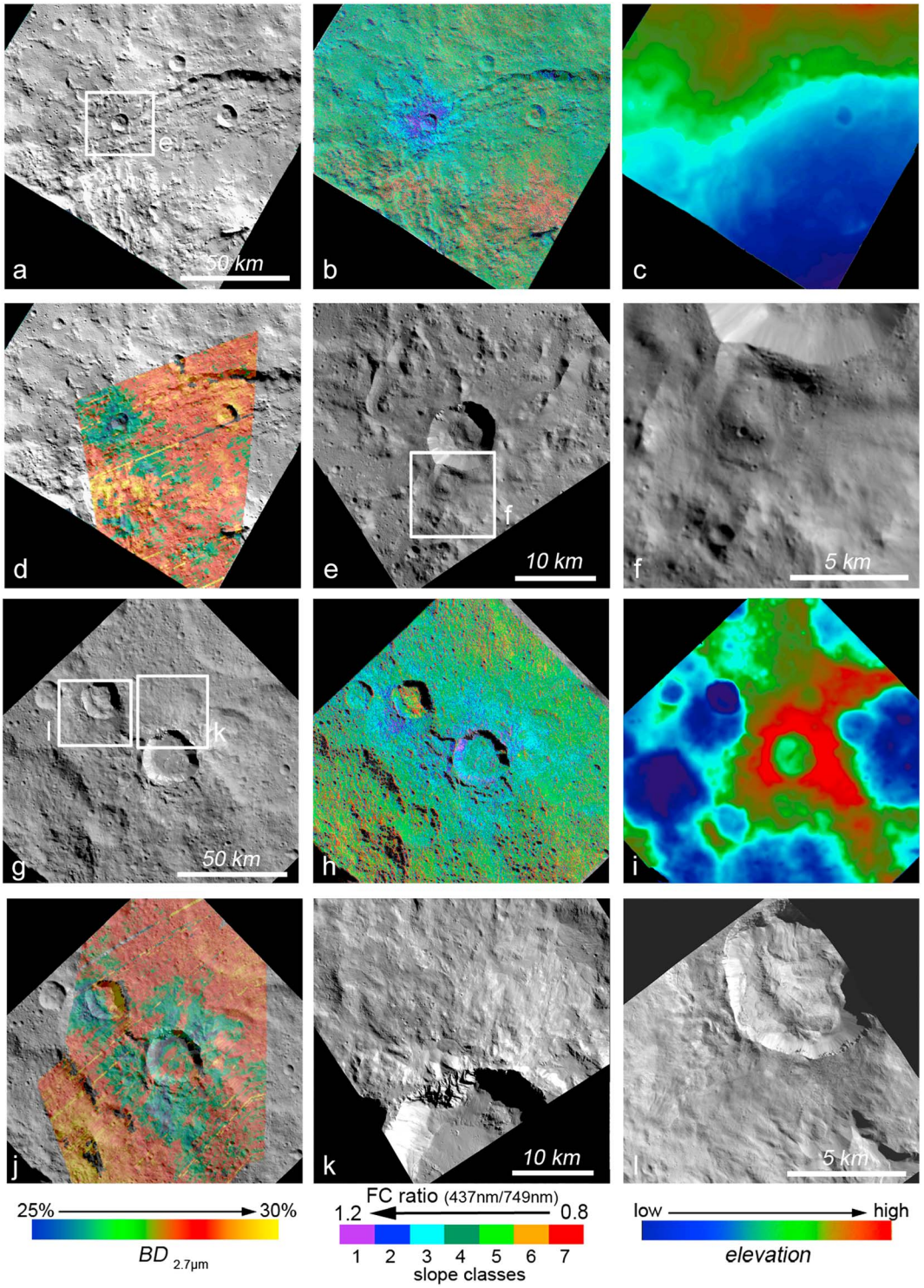

Figure 3. Type localities of blue material: (a) FC image of Tawals with the corresponding (b) slope classification map like Figure 1, (c) DTM, (d) VIR BD 2.7 μm map, and (e and f) close up images of blue ejecta material, (g) FC image of Juling and Kupalo and the corresponding (h) slope classification map like Figure 1, (i) DTM, (j) VIR BD 2.7 μm map, and (k and l) close up images of blue ejecta material.

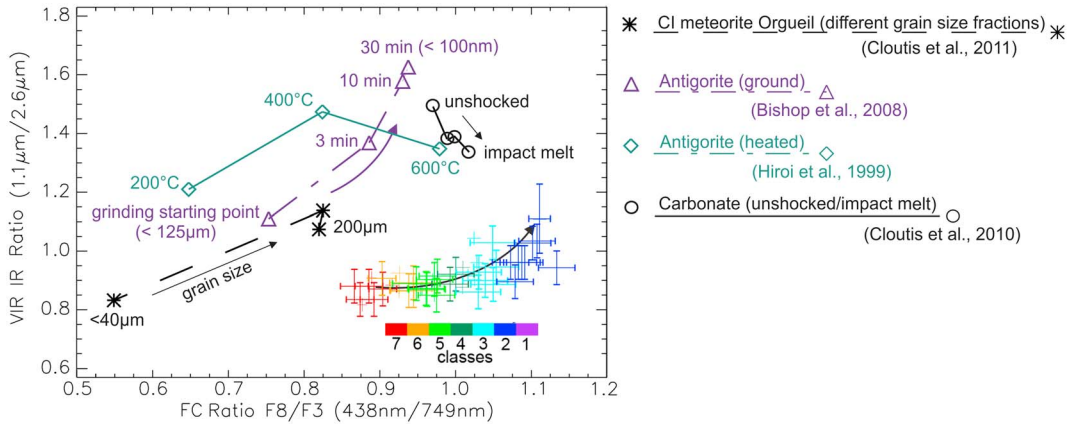

Figure 4. Comparison of average FC ratio (like F8/F3) and VIR ratio (1.1 μm/2.5 μm) derived for type localities of the slope classes indicated in Figure 1 to the corresponding ratios derived for spectra of analog materials (RELAB spectral library) that have been reported to show spectral bluing in the visible wavelength range due to changes in the physical surface properties such as grain size changes/crystallization and temperature.

In the area of *Haulani* (Figures 2g–2l), all identified spectral slope classes could be mapped. Blue areas are associated with (bright) ejecta deposits. In contrast to Oxo, crater walls are not completely covered with blue material. The crater floor and the southeastern crater wall are partly covered with reddish material, which may represent redeposited slumping material from the southern topographic heights. The blue material rather becomes apparent in morphologically smooth areas with flow features originating from a mountainous region in the center of the crater that cover the preexisting surface [*Krohn et al.*, 2016]. The albedo of the blue areas is with relatively high (~0.067) [*Schmedemann et al.*, 2016] and the absorptions at 2.7 μm and 3.1 μm are weaker for Haulani compared to the surroundings (Figure 2j). The weakest absorptions are confined to the crater itself (except the mass wasting material close to the southern crater rim) but are also weak in the vicinity of the ejecta and flows.

Impact crater Tawals (Figures 3a–3f) is one of the few impact craters that do not show any bright ejecta deposits in FC images. Tawals is located directly at the rim of impact basin Urvara. The blue material dominates the crater as well as the ejecta. Boulders can be recognized in the ejecta material close to the crater rim, which transform into smooth material with growing distance from the crater. Although the overall albedo of Tawals (~2%) is lower than the albedos of Haulani and Oxo, the VIR-derived spectral slope of Tawals is similar to the spectral slope of Haulani (slope class 2). Urvara itself shows red-sloped terrain (class 7), which clearly marks geologically older, rough, and heavily cratered terrain. Only few impact craters on Ceres show a distinct red-colored crater floor and bluish ejecta like the small impact crater Juling (diameter: 20 km, 35.9°S/168.5°E) (Figures 3g–3l). Juling, however, is located on a topographic slope and is not surrounded by a distinctly elevated crater rim like its neighbor Kupalo (diameter: 26 km, 39.5°S/173.2°E). Similar to what we observed in Haulani, slumping from the topographically high standing and geologically old heavily cratered terrain could have occurred here.

4. Comparison to Other Planetary Objects and Materials

Although blue slopes are not common in the spectra of planetary bodies and terrestrial analog materials, a few observations have been reported, where a bluing effect as seen in the spectra of Ceres could be observed. In Figure 4 the FC-derived ratio values (F8/F3 ratio) measured for type localities on Ceres indicated in Figure 1 are shown in correlation to the corresponding VIR-derived ratio values using the VIR channels centered at 1.1 and 2.5 μm. A distinct "bluing" is apparent in the visible wavelength range (F8/F3 ratio) when moving from the regions of the red to the blue slope class. A weaker but similar trend is still recognizable in the infrared wavelength region illustrated by the 1.1/2.5 μm ratio. In this plot also corresponding ratio values derived from available spectra of relevant analog material provided by the RELAB library (http://www.planetary.brown.edu/relab/) and which have been reported to exhibit a bluing effect are shown.

B-type asteroids like Pallas and its family members often show a blue spectral slope from ~0.5 μm to 1.1 μm [*Clark et al*., 2010]. CM and CI carbonaceous chondrites (mainly composed of phyllosilicates and iron oxides like magnetite) are believed to be a relevant meteoritic analog for B-type asteroids as well as for Ceres [*Clark et al*., 2010; *Johnson and Fanale*, 1973]. Darker CI spectra (visible albedo <10%) are generally correlated with a bluer spectral slope and reduced silicate absorption band depths, a behavior that could be associated with an increasing abundance of magnetite and graphite [*Cloutis et al*., 2011; *Johnson and Fanale*, 1973]. This, however, is contrary to what can be seen on Ceres's surface. Although, dark material is used to explain the extremely low albedo of Ceres [*De Sanctis et al*., 2015; *Rivkin et al*., 2010], it cannot explain the mostly visually brighter bluer material (Figure 1). Only the small crater Tawals (Figure 3) shows a blue slope and a lower albedo than the surroundings. The lower albedo possibly implies a higher concentration of a visually dark, possibly carbon-rich surface compound [*Hendrix et al*., 2016] in the crater material, supporting that the blue slope might not be connected to the actual composition. However, increasing grain size and/or abundance of amorphous/poorly crystalline material have also been discussed leading to a bluer slope [*Cloutis et al*., 2011]. Ratio values derived from laboratory spectra of different grain size fractions (from <40 μm to 200 μm) of CI meteorite Orgueil (discussed in *Cloutis et al*. [2011]) show a similar trend to the Ceres-derived ratio values (Figure 4). The offset between the actual ratio values derived for Ceres and Orgueil might not speak against this relationship, but could be caused by different spatial resolutions (remote versus laboratory data) as well as slight differences in the specific composition of Ceres's surface.

Similar bluing effects have been also observed in spectra of phyllosilicates, the most ubiquitous surface compound on Ceres's surface [*Ammannito et al*., 2016; *De Sanctis et al*., 2015, 2016]. Laboratory experiments performed by *Bishop et al*. [2008] show that antigorite exhibits a spectral slope which turns blue with grinding of the sample (Figure 4) with a remarkably similar trend as observed for the surface material on Ceres. The authors describe that amorphous material is formed and ultrafine (~50–100 nm in size) grains that strongly stick together forming larger agglomerates (tens of micrometer in size) due to the mechanical stress caused by the grinding process. Thus, the spectral signature of the sample rather reflects the properties of the amorphous material and/or aggregates than individual grains [*Cooper and Mustard*, 1999], and the spectral bluing is caused by either relatively larger aggregates and/or a higher abundance of amorphous material. Intriguingly, blue-sloped phyllosilicates are also characterized by weaker OH-absorptions at 1.4, 1.9, ~2.2 μm, and 2.73 μm in hydrated and/or hydroxylated materials caused by changes in the ratio of scattering to absorption with grain size [*Bishop et al*., 2008; *Cooper and Mustard*, 1999], which has also been observed on Ceres [*Ammannito et al*., 2016]. Mechanical brecciation, grinding, and amorphization/melting of surface material also happens during an impact event [*French*, 1998]. Thus, agglomerates of ultrafine or amorphous phyllosilicate grains could offer an explanation for the bluish regions in more than one way and indicating physical rather than chemical changes between the reddish and bluish material of Ceres's surface.

In addition, bluer spectral slopes apparently are somewhat positively correlated with increasing thermal metamorphism in both naturally heated and laboratory-heated spectra of carbonaceous chondrites (ATCC chondrites) probably mainly resulting in the dehydration of the phyllosilicates, increasing grain size and/or production of abundant amorphous material [*Cloutis et al*., 2012, 2013]. An appearance of a blue spectral slope in spectra of phyllosilicates has also been noted when heated [*Hiroi and Zolensky*, 1999] and has also been observed in terrestrial carbonate-rich impact melt breccia [*Cloutis et al*., 2010; *Craig et al*., 2009], which are shown in Figure 4. However, their trend with respect to a spectral blue slope shows higher discrepancies from the Ceres data than the measurements discussed above. The "bluing" in the spectra of antigorite occurs due to heating up to a temperature of ~400°C. At higher temperature the trend reverses. Spectra of shocked/melted carbonates shows a bluing effect similar to what is seen in the visible part of the Ceres spectra (FC ratio in Figure 4), but differs significantly from the ratios measured in the VIR-IR spectra. Thus, grain size effects and an increasing amount of amorphous material tend to offer the best explanation for Ceres's blue material and might not be limited to phyllosilicates alone.

Bluish material has been also observed on other planetary bodies like the icy satellites of Jupiter and Saturn associated with relatively large-grained fresh ice recently exposed on the surface [*Jaumann et al*., 2008; *Stephan*, 2006; *Stephan et al*., 2010, 2012]. A contribution of H_2O ice could explain the higher visible albedo of the blue material. However, it does not explain why areas that do not show any hint of H_2O ice exhibit a similar steep blue slope. Recent observations by *Dawn*'s GRaND instrument favor extended ice deposits in

Ceres subsurface [*Prettyman et al*., 2017]. Oxo definitely indicates H_2O ice in Ceres's subsurface supporting the existence of H_2O ice close to the surface. However, H_2O ice only may be stabilize in the near surface at high latitudes [*Fanale and Salvail*, 1989; *Hayne and Aharonson*, 2016]. *Poch et al*. [2016] showed that smectites mixed with H_2O ice show a distinctly blue spectral slope (in comparison to a distinctly red slope of pure smectite) and that the blue slope remains after the sublimation of H_2O ice, whereas the absorptions of H_2O ice at 1.5 and 2 μm completely disappear. These experiments, however, appear rather relevant for a cometary surface as the authors intended. On Ceres, however, the bluish material is clearly related to impact processes [*Schröder et al*., 2017]. Impact processes are known to instantaneously remove large quantities of H_2O ice existing in the subsurface [*French*, 1998], and it is not clear how pores of already vaporized H_2O-ice particles should remain existent in the emplaced ejecta deposits during the impact process. Further, the sublimation of H_2O ice causing the blue slope does not explain why the blue slope is related to a weaker 2.7 μm signature. However, *Poch et al*. [2016] explain their observation by a peculiar scattering behavior caused by nanometer-sized grains [*Brown*, 2014], which has been also observed on the icy satellites of Saturn [*Clark et al*., 2012]. Thus, a similar behavior is apparently not limited to a specific composition but to specific physical surface properties.

Finally, *Hendrix et al*. [2016] proposed sulfur and SO_2, with the latter also exhibiting a bluish visible signal, to be existent in addition to phyllosilicates and a carbon-rich material on Ceres based on UV data of the Hubble Space Telescope and describe an increasing content in SO_2 toward northern high latitudes. SO_2 exhibits diagnostic absorptions in the infrared wavelength region detected by VIR such as a strong absorption near 4.07 μm [*Nash and Betts*, 1995]. Although it is an intriguing idea that sulfur compounds exist on Ceres's surface, VIR did not identify any sulfur compounds so far.

5. Discussion of the Nature of the Bluish Material

In comparison with the geology/morphology of Ceres, it is clearly evident that the distribution of blue-sloped material as well as the occurrence of a weaker absorption at 2.73 μm is associated with fresh impact craters. Thus, either this blue-sloped material exists in the subsurface and has been exposed due to impact events or it has been formed during the impact processes. Physical alteration such as amorphization and aggregation of small-grained phyllosilicate-rich material and even heating up and melting the impacted surface material to moderate temperatures is expected in case of low-velocity impact events, which could explain the observed blue spectral slope. Especially, more melt-rich material usually emplaced during the terminal stages of crater formation conforms to the observed morphology and character of the blue-sloped ejecta deposits, which are often accompanied by lobate shapes indicating melted material flown across the surface [*Krohn et al*., 2016]. Impact melt can form ponds on a crater's floor but also can occur on the interior crater walls as well as beyond the crater rim. The final morphology and character of the ejecta deposits is affected by several factors including the volatile content and physical properties of the uppermost target rocks. In particular, impacts into phyllosilicates and carbonates, both materials detected on Ceres, which unlike crystalline rocks may be more porous and volatile-rich, are expected to produce more melt than impacts into denser crystalline rocks, and to form aggregates that are ejected from the crater with a plume of expanding volatiles [*French*, 1998]. Material melted and vaporized during the impact event may be ejected to significant distances at high velocities, which could also explain the linear features observed on Ceres [*Buczkowski et al*., 2016].

Our results are consistent with the work of *Schmedemann et al*. [2016] and *Krohn et al*. [2016] who have determined the blue-sloped material to be the youngest material on Ceres's surface and interpreted the association of flow features with impact craters as indication for highly fluidized material/impact melt. The theory of an impact-triggered altering of the physical properties of Ceres's surface material as the cause of the blue slope would offer also an explanation for the linear features composed of ejected material described by *Buczkowski et al*. [2016] but also for the existence of Ahuna Mons [*Ruesch et al*., 2016; *Zambon et al*., 2016]—the only location on Ceres interpreted as a viscous cryovolcanic dome with molten material uprising onto Ceres surface. The recrystallization of the amorphous surface material and/or reversal of the agglutination process then start due to diurnal temperature variations and micrometeoritic impacts forming a regolith layer of fine-grained phyllosilicate dust resulting in a reddening of the spectral slope.

Acknowledgments

We thank the *Dawn* team for the development, cruise, orbital insertion, and operations of the *Dawn* spacecraft at Ceres. Portions of this work were performed at the DLR Institute of Planetary Research, at the Jet Propulsion Laboratory (JPL) under contract with NASA, as well as at the National Institute for Astrophysics (Rome, Italy). *Dawn* data are archived with the NASA Planetary Data System (http://sbn.pds.nasa.gov/).

References

Ammannito, E., et al. (2016), Distribution of phyllosilicates on the surface of Ceres, *Science*, *353*(6303), doi:10.1126/science.aaf4279.

Bishop, J. L., M. D. Dyar, E. C. Sklute, and A. Drief (2008), Physical alteration of antigorite: A Mössbauer spectroscopy, reflectance spectroscopy and TEM study with applications to Mars, *Clay Miner.*, *43*(1), 55–67.

Brown, A. J. (2014), Spectral bluing induced by small particles under the Mie and Rayleigh regimes, *Icarus*, *239*, 85–95.

Buczkowski, D. L., et al. (2016), The geomorphology of Ceres, *Science*, *353*, doi:10.1126/science.aaf4332.

Clark, B. E., et al. (2010), Spectroscopy of B-type asteroids: Subgroups and meteorite analogs, *J. Geophys. Res.*, *115*, E06005, doi:10.1029/2009JE003478.

Clark, R. N., et al. (2012), The surface composition of Iapetus: Mapping results from Cassini VIMS, *Icarus*, *218*(2), 831–860.

Cloutis, E. A., S. E. Grasby, W. M. Last, R. Léveillé, G. R. Osinski, and B. L. Sherriff (2010), Spectral reflectance properties of carbonates from terrestrial analogue environments: Implications for Mars, *Planet. Space Sci.*, *58*, 522–537.

Cloutis, E. A., T. Hiroi, M. J. Gaffey, C. M. O. D. Alexander, and P. Mann (2011), Spectral reflectance properties of carbonaceous chondrites: 1. CI chondrites, *Icarus*, *212*(1), 180–209.

Cloutis, E. A., P. Hudon, T. Hiroi, and M. J. Gaffey (2012), Spectral reflectance properties of carbonaceous chondrites 4: Aqueously altered and thermally metamorphosed meteorites, *Icarus*, *220*(2), 586–617.

Cloutis, E. A., P. Hudon, T. Hiroi, M. J. Gaffey, P. Mann, C. M. O. D. Alexander, J. F. Bell, and B. E. Clark (2013), Possible causes of blue slopes (~0.5–2.5 μm) in carbonaceous chondrite spectra, Lunar Planet. Sci. Conf., p. 1550.

Combe, J.-P., et al. (2016), Detection of local H_2O exposed at the surface of Ceres, *Science*, *353*(6303).

Cooper, C. D., and J. F. Mustard (1999), Effects of very fine particle size on reflectance spectra of smectite and palagonitic soil, *Icarus*, *142*, 557–570.

Craig, M. A., G. R. Osinski, R. L. Flemming, and E. A. Cloutis (2009), UV-Vis-NIR reflectance spectra of shocked carbonates from the Haughton impact structure, Devon Island, Canada: 0.35–2.5 μm; implications for carbonate identification on Mars, Lunar Planet. Sci. Conf.

De Sanctis, M. C., et al. (2011), The VIR spectrometer, *Space Sci. Rev.*, *163*, 329–369.

De Sanctis, M. C., et al. (2015), Ammoniated phyllosilicates with a likely outer solar system origin on (1) Ceres, *Nature*, *528*, 241–244.

De Sanctis, M. C., et al. (2016), Bright carbonate deposits as evidence of aqueous alteration on (1) Ceres, *Nature*, *536*, 54–57.

Fanale, F. P., and J. R. Salvail (1989), The water regime of asteroid (1) Ceres, *Icarus*, *82*, 97–110.

French, B. M. (1998), Traces of catastrophe: A handbook of shock-metamorphic effects in terrestrial meteorite impact structures, LPI Contribution No. 954, Lunar and Planetary Institute, 120 pp., Houston, Tex.

Hayne, P. O., and O. Aharonson (2016), Ice sublimation, outgassing, and melting on Ceres: Models and observations, Lunar Planet. Sci. Conf., p. 2736.

Hendrix, A. R., F. Vilas, and J.-Y. Li (2016), Ceres: Sulfur deposits and graphitized carbon, *Geophys. Res. Lett.*, *43*, 8920–8927, doi:10.1002/2016GL070240.

Hiesinger, H., et al. (2016), Cratering on Ceres: Implications for its crust and evolution, *Science*, *353*, doi:10.1126/science.aaf4759.

Hiroi, T., and M. E. Zolensky (1999), UV-Vis-NIR absorption features of heated phyllosilicates as remote-sensing clues of thermal histories of primitive asteroids, *Antarct. Meteorite Res.*, *12*, 108.

Jaumann, R., et al. (2008), Distribution of icy particles across Enceladus' surface as derived from Cassini-VIMS measurements, *Icarus*, *193*(2), 407–419.

Jaumann, R., et al. (2016), Age-dependent morphological and compositional variations on Ceres, Lunar Planet. Sci. Conf., p. 1455.

Johnson, T. V., and F. P. Fanale (1973), Optical properties of carbonaceous chondrites and their relationship to asteroids, *J. Geophys. Res.*, *78*, 8507–8518, doi:10.1029/JB078i035p08507.

Krohn, K., et al. (2016), Cryogenic flow features on Ceres: Implications for crater-related cryovolcanism, *Geophys. Res. Lett.*, *43*, 11,994–12,003, doi:10.1002/2016GL070370.

Nash, D. B., and B. H. Betts (1995), Laboratory infrared spectra (2.3–23 μm) of SO_2 phases: Applications to Io surface analysis, *Icarus*, *117*, 402–419.

Poch, O., A. Pommerol, B. Jost, N. Carrasco, C. Szopa, and N. Thomas (2016), Sublimation of water ice mixed with silicates and tholins: Evolution of surface texture and reflectance spectra, with implications for comets, *Icarus*, *267*, 154–173.

Prettyman, T. H., et al. (2017), Extensive water ice within Ceres' aqueously altered regolith: Evidence from nuclear spectroscopy, *Science*, *355*(6320), 55–59.

Preusker, F., F. Scholten, K.-D. Matz, S. Elgner, R. Jaumann, T. Roatsch, S. P. Joy, C. A. Polanskey, C. A. Raymond, and C. T. Russell (2016), *Dawn* at Ceres—Shape model and rotational state, Lunar Planet. Sci. Conf., p. 1954.

Rivkin, A. S., J.-Y. Li, R. E. Milliken, L. F. Lim, A. J. Lovell, B. E. Schmidt, L. A. McFadden, and B. A. Cohen (2010), The surface composition of Ceres, *Space Sci. Rev.*, *163*(1–4), 95–116.

Roatsch, T., E. Kersten, K.-D. Matz, F. Preusker, F. Scholten, R. Jaumann, C. A. Raymond, and C. T. Russell (2016), High-resolution Ceres high altitude mapping orbit atlas derived from *Dawn* Framing Camera images, *Planet. Space Sci.*, *129*, 103–107.

Ruesch, O., et al. (2016), Cryovolcanism on Ceres, *Science*, *353*(6303), doi:10.1126/science.aaf4286.

Schenk, P. M., and W. B. McKinnon (1991), Dark-ray and dark-floor craters on Ganymede, and the provenance of large impactors in the Jovian system, *Icarus*, *89*, 318–346.

Schmedemann, N., et al. (2016), Timing of optical maturation of recently exposed material on Ceres, *Geophys. Res. Lett.*, *43*, 11,987–11,993, doi:10.1002/2016GL071143.

Schröder, S. E., et al. (2017), Resolved spectrophotometric properties of the Ceres surface from Dawn Framing Camera images, *Icarus*, *288*, 201–225.

Sierks, H., et al. (2011), The *Dawn* Framing Camera, *Space Sci. Rev.*, *163*, 263–327.

Stephan, K. (2006), Chemisch-physikalische Zusammensetzung der Ganymedoberfläche: Zusammenhänge mit geologischen Strukturen und deren Gestaltungsprozessen [in German], PhD Dissertation thesis.

Stephan, K., et al. (2010), Dione's spectral and geological properties, *Icarus*, *206*(2), 631–652.

Stephan, K., et al. (2012), The Saturnian satellite Rhea as seen by Cassini VIMS, *Planet. Space Sci.*, *61*(1), 142–160.

Tosi, F., et al. (2014), Thermal measurements of dark and bright surface features on Vesta as derived from *Dawn*/VIR, *Icarus*, *240*, 36–57.

Zambon, F., et al. (2016), Mineralogy of Ahuna Mons on Ceres surface, AAS/Division for Planet. Sci. Meeting Abstr.